

# Forward Jets in Deep Inelastic Scattering at HERA

A. De Roeck

Deutsches Elektronen Synchrotron, DESY  
Hamburg, Germany

On behalf of the H1 and ZEUS collaborations

## Abstract

The rate of forward jets, i.e. jets with a small angle with respect to the proton direction, has been measured in deep inelastic scattering events at the  $ep$  collider HERA. Such a measurement has been proposed as a signature for observing BFKL dynamics. An inclusive jet cross section measurement is presented for jets in the target region of the Breit Frame.

## Résumé

Le taux d'événements avec un jet de particules vers l'avant, c.a.d faisant un petit angle avec la direction du proton incident a été mesuré dans les collisions profondément inélastiques auprès du collisionneur electron-proton HERA. Ce type de mesure a été proposé pour mettre en évidence une dynamique BFKL. La mesure de la section efficace inclusive de production de jet dans la région du résidu du proton est présentée dans le référentiel de Breit.

## 1. Introduction

The electron-proton collider HERA has opened new kinematical regions for the study of deep inelastic scattering (DIS): the regions of large four-momentum transfer  $Q^2$  (up to  $Q^2 \approx 10^4 \text{ GeV}^2$ ) and small Bjorken- $x$  (down to  $x \approx 10^{-4}$ ). It has been suggested [1] that the small  $x$  region may be sensitive to new dynamic features of QCD. The ZEUS and H1 collaborations have observed [2, 3] that the proton structure function  $F_2$  exhibits a strong rise towards small Bjorken- $x$ . This rise has caused much debate on whether the HERA data are still in a regime where the QCD evolution of the parton densities can be described by the DGLAP (Dokshitzer-Gribov-Lipatov-Altarelli-Parisi) [4] evolution equations, or whether they extend into a new regime where the QCD dynamics is described by the BFKL (Balitsky-Fadin-Kuraev-Lipatov) [5] evolution equation. The BFKL evolution equation is expected to become

applicable in the small  $x$  region, since it resums all leading  $\alpha_s \ln 1/x$  terms in the perturbative expansion, in contrast to the DGLAP equation. Present  $F_2$  measurements do not yet allow to discriminate between BFKL and conventional DGLAP dynamics [6, 7], and are perhaps too inclusive a measurement to be a sensitive discriminator. Hadronic final states are expected to give additional information and to be more sensitive to the parton evolution [8, 9, 10]. In this paper we study jet production in the region away from the struck quark, towards the proton remnant. Since at HERA the proton direction is called "forward" direction, these jets are termed "forward jets".

The data used in these analyses were collected by the H1 and ZEUS experiments in 1993 at HERA, where electrons of energy  $E_e = 26.7 \text{ GeV}$  collide with protons of energy  $E_p = 820 \text{ GeV}$ , resulting in a total centre of mass energy of  $\sqrt{s} = 296 \text{ GeV}$ . The data correspond to an integrated luminosity of  $320 \text{ nb}^{-1}$  and  $540 \text{ nb}^{-1}$

for H1 and ZEUS, respectively.

## 2. BFKL and DGLAP dynamics

For events at low  $x$ , hadron production in the region between the current jet and the proton remnant is expected to be sensitive to the effects of the BFKL or DGLAP dynamics. At lowest order the BFKL and DGLAP evolution equations effectively resum the leading logarithmic  $\alpha_s \ln 1/x$  or  $\alpha_s \ln Q^2$  contributions respectively. In an axial gauge this amounts to a resummation of ladder diagrams of the type shown in Fig. 1. This shows that before a quark is struck by the virtual photon, a cascade of partons may be emitted. The fraction of the proton momentum carried by the emitted partons,  $x_i$ , and their transverse momenta,  $k_{Ti}$ , are indicated in the figure. In the leading log DGLAP scheme this parton cascade follows a strong ordering in transverse momentum  $k_{Tn}^2 \gg k_{Tn-1}^2 \gg \dots \gg k_{T1}^2$ , while there is only a soft (kinematical) ordering for the fractional momentum  $x_n < x_{n-1} < \dots < x_1$ . In the BFKL scheme the cascade follows a strong ordering in fractional momentum  $x_n \ll x_{n-1} \ll \dots \ll x_1$ , while there is no ordering in transverse momentum [11]. The transverse momentum follows a kind of random walk in  $k_T$  space: the value of  $k_{Ti}$  is close to that of  $k_{T(i-1)}$ , but it can be both larger or smaller [12].

A proposed signature of the BFKL dynamics is the rate of jets with transverse momentum  $k_{Tjet} \approx Q$  and the momentum fraction of the jet,  $x_{jet} = E_{jet}/E_p$ , large compared with Bjorken- $x$  [9, 10, 13]. Here  $E_{jet}$  and  $E_p$  are the energies of the jet and the incoming proton respectively. Due to the strong ordering in the DGLAP evolution, the condition  $k_{Tjet} \approx Q$  suppresses the phase space for jet production. However jet production from BFKL evolution is governed by the ratio  $x_{jet}/x$ , which is large. Hence the rate of events with a jet satisfying the selection is predicted to be higher for the BFKL than for the DGLAP scenario.

The jet rates will be compared with predictions from Monte Carlo models which are based on QCD phenomenology. In this report we consider two of the currently available Monte Carlo programs: the MEPS (Matrix Elements plus Parton Showers) and CDM (Colour Dipole Model) models. The CDM model [14] provides an implementation of the colour dipole model of a chain of independently radiating dipoles formed by emitted gluons [15]. Photon-gluon fusion events are not described by this picture and are added at a rate given by the QCD matrix elements [16]. The CDM description of gluon emission is similar to that of the BFKL evolution, because the gluons emitted by the dipoles do not obey strong ordering in  $k_T$  [17]. The CDM does not explicitly make use of the BFKL evolution equation, however. The MEPS model is an option of

the LEPTO generator [16] based on DGLAP dynamics. MEPS incorporates the QCD matrix elements up to first order, with additional soft emissions generated by adding leading log parton showers. The emitted partons are strongly ordered in  $k_T$ . Both Monte Carlo programs use the Lund string model [18] for hadronizing the partonic final state.

Apart from Monte Carlo predictions, analytical calculations have been performed for this process [10]. Recently a new calculation became available [21], tailored to the kinematical range selected by the measurements. These calculations are so far at the parton level.

The H1 analysis presented in this paper discusses the measurement made in the kinematical range of  $x_{jet} \gg x$  and  $k_{Tjet} \sim Q$ . ZEUS presents a measurement of the inclusive jet cross section for jets in the current and target hemisphere, as an initial study for testing BFKL dynamics in the forward region.

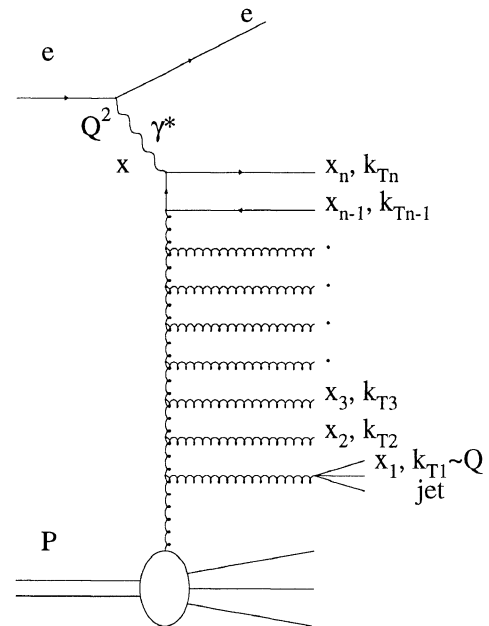
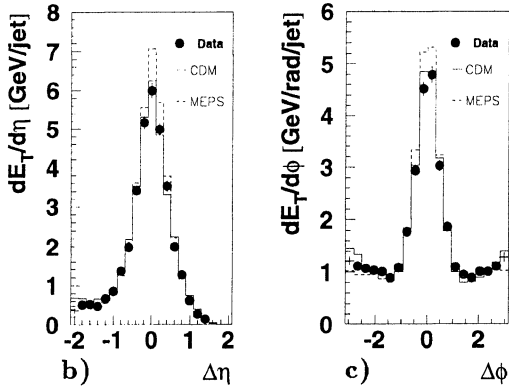


Figure 1. Parton evolution in the ladder approximation. The selection of forward jets in DIS events is illustrated.

## 3. Events with a forward jet (H1)

In this section the cross section of the process given in Fig. 1 is studied. For this analysis DIS events with  $Q^2 < 100 \text{ GeV}^2$  are used, in which the scattered electron is observed in the backward electromagnetic calorimeter of the experiment [19]. The kinematic variables are determined using information from the scattered electron:  $Q^2 = 4 E_e E'_e \cos^2(\theta_e/2)$  and  $y =$

forward  
jet  
a)



**Figure 2.** a) DIS event with a forward jet in the H1 detector. The protons are incident from the right, electrons from the left. The scattered electron is detected in the backward electromagnetic calorimeter (BEMC) with an angle of  $166^\circ$  and an energy of 18.9 GeV. The forward jet is observed in the liquid argon calorimeter and has an angle  $\theta_{jet} = 11^\circ$  and an energy  $E_{jet} = 65$  GeV. Averaged over all events with a selected forward jet, the transverse energy flow around the forward jet axis is shown in b) as a function of  $\Delta\eta$ , integrated over  $|\Delta\phi| < 1.0$  and in c) as a function of  $\Delta\phi$ , integrated over  $|\Delta\eta| < 1.0$ . Here  $\Delta\eta$  and  $\Delta\phi$  are measured with respect to the reconstructed jet axis.

$1 - (E'_e/E_e) \cdot \sin^2(\theta_e/2)$ . The scaling variable  $x$  is then derived via  $x = Q^2/(ys)$ .

DIS events are selected in the following way. The scattered electron must have an energy  $E'_e$  larger than 12 GeV and a polar angle  $\theta_e$  below  $173^\circ$  in order to ensure a high trigger efficiency and a small photoproduction background [3]. Further reduction of photoproduction background and the removal of events in which an energetic photon is radiated off the incoming electron (radiative events) is achieved by requiring  $\sum_j (E_j - p_{z,j}) > 30$  GeV [3], where the sum includes all particles  $j$  of the event. Here  $E_j$  is the energy and  $p_{z,j}$  the longitudinal momentum component of a particle. In addition the requirement  $y > 0.1$  was imposed to ensure that the jet of the struck quark is well within the central region of the detector and (for non-radiative events) is

† Polar angles are defined with respect to the proton direction

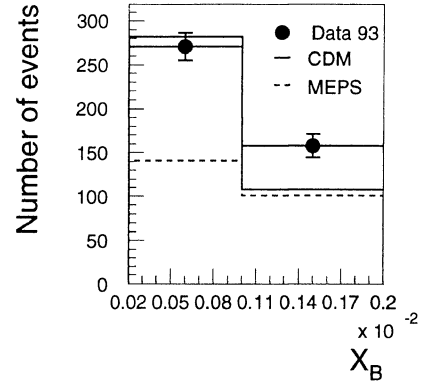


**Figure 3.** The number of observed DIS events with a selected forward jet (statistical errors only), corrected for radiative events faking this signal, compared to predictions of the CDM and MEPS model.

$x$ range (* $10^{-4}$ )	data events	MEPS events	CDM events	$\sigma(ep \rightarrow jet + X)$ (pb)
2 – 10	271	141	282	$709 \pm 42 \pm 166$
10 – 20	158	101	108	$475 \pm 39 \pm 110$

**Table 1.** Numbers of observed DIS events with a selected forward jet, corrected for radiative events faking this signature. These may be directly compared with the expectations from the Monte Carlo models. The measured cross section  $ep \rightarrow jet + X$  for forward jets is also given. The errors reflect the statistical and systematic uncertainties.

expected to have a jet angle larger than  $60^\circ$ .

DIS events are studied at small  $x$  which have a jet with large  $x_{jet}$  [20]. A cone algorithm is used to find jets, requiring an  $E_T$  larger than 5 GeV in a cone of radius  $R = \sqrt{\Delta\eta^2 + \Delta\phi^2} = 1.0$  in the space of pseudo-rapidity  $\eta$  and azimuthal angle  $\phi$  in the HERA frame of reference. In this sample of DIS events with  $Q^2 \approx 20$  GeV<sup>2</sup> and  $2 \cdot 10^{-4} < x < 2 \cdot 10^{-3}$  we have counted events which have a “forward” jet defined by  $x_{jet} > 0.025$ ,  $0.5 < p_{Tjet}^2/Q^2 < 4$ ,  $6^\circ < \theta_{jet} < 20^\circ$  and  $p_{Tjet} > 5$  GeV, where  $p_{Tjet}$  is the transverse momentum of the jet. A typical event with a high energy forward jet is shown in Fig. 2a. The transverse energy flow around the forward jet axis, averaged over all selected events, is shown versus  $\eta$  and  $\phi$  in Figs. 2b and 2c. Distinct jet profiles are observed, which are well described by the Monte Carlo models.

The resulting number of events observed with at least one forward jet in the kinematical region  $160^\circ < \theta_e < 173^\circ$  and  $E'_e > 12$  GeV is shown in Fig.3 and given in Table 1 and compared to expectations of the MEPS and CDM models after detector simulation. The data are corrected for photoproduction background and radiative events, which due to the changed kinematics at the hadron vertex can eject a jet in the forward

direction. About 4% of the data events were found to contain two forward jets. In the kinematic range studied here the CDM generally describes the data better than the MEPS model. However, increasing the  $x_{jet}$  cut from 0.025 to 0.05 reduces the total number of events with forward jets to 46 for CDM, to 77 for MEPS and to 105 for the data, hence CDM does not describe the rate of high energy jets.

The measured cross section for forward jets satisfying the cuts given above is also presented in Table 1. It has been corrected for detector effects using the CDM. The systematic errors include effects from DIS event selection, the calorimeter energy scale (5%), the jet angle bias (10 mrad), the proton structure function, and a global normalization uncertainty of 4.5%. Event pile-up effects were found to be negligible. The systematic errors on the two data points are largely correlated. The ratio of the jet cross section for the low  $x$  to the high  $x$  bin is  $1.49 \pm 0.25$ .

The precision of the data does not yet allow a firm conclusion to be drawn. We note, however, that the forward jet cross section is larger in the low  $x$  bin than in the high  $x$  bin. This is expected from BFKL dynamics as a recent analytical calculation [21] at the parton level demonstrates: in the kinematical region selected the ratio of the cross sections in the low  $x$  bin to high  $x$  bin is 1.62 for a calculation including BFKL evolution, compared to 1.03 for a calculation without gluon emission from the ladder in Fig. 1.

#### 4. Inclusive jet production cross sections (ZEUS)

In this analysis the inclusive jet production cross section is measured separately in both hemispheres of the Breit frame. In this frame the virtual photon and the proton are collinear and the exchanged current is entirely space-like, having just a  $z$ -component of momentum  $-Q$ . In the simple QPM picture the convention is used that the incident parton approaches with momentum  $+Q/2$ , absorbs the photon, and leaves with momentum  $-Q/2$ , in what is called the current hemisphere; the other one is called the target hemisphere.

Deep inelastic scattering events for this analysis are selected in the ZEUS detector [22] by requiring an identified electron with transverse energy  $E_T > 5$  GeV (hence  $Q^2 > 25$  GeV<sup>2</sup>),  $y < 0.95$ ,  $y_{JB} > 0.08$  with  $y_{JB} = \sum_h (E_h - p_{z,h})/2E_e$ , where the sum includes all hadrons  $h$ . To reduce radiation and photoproduction background a cut  $\sum_j E_j - p_{z,j} > 35$  GeV is applied (sum includes all particles  $j$ ).

Jets are identified in the data with the  $k_T$  jet finding algorithm [23], using the E-scheme and a  $y_{cut} = 0.5$ . The energies of the jets have been corrected for losses using a technique based on energy balance in

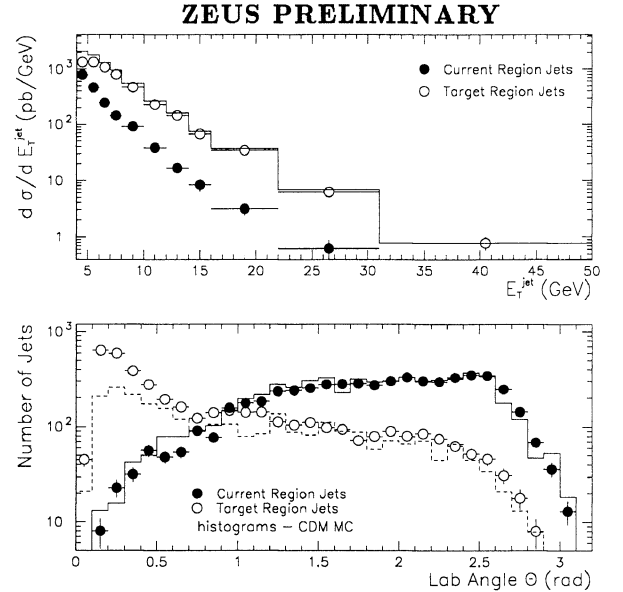


**Figure 4.** (top) The cross section  $d\sigma/dE_T$  and (bottom) the laboratory angular distribution of jets detected either in the Breit current or target hemisphere.

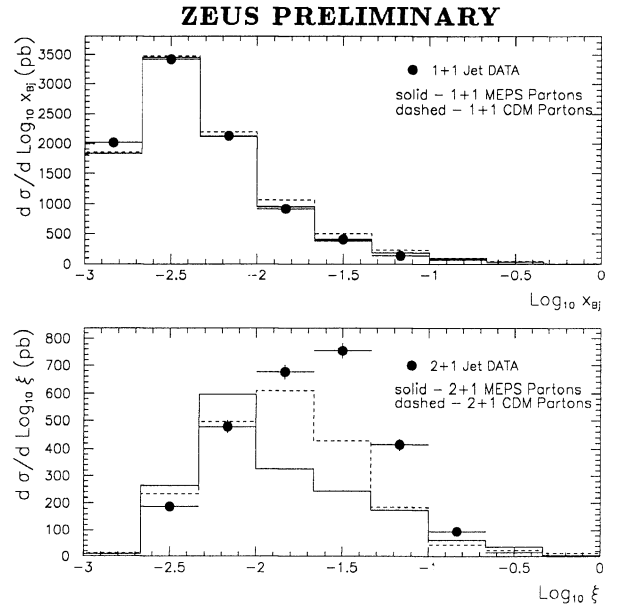


**Figure 5.** The cross section for jet events as function of the target momentum fraction, for (top) 1+1 jet events and (bottom) 2+1 jet events.

1-jet events. Monte Carlo studies show that in the chosen kinematical range the rates of the measured jets correspond closely to the rates of the parton jets. Henceforth the data will be compared with parton jet Monte Carlo calculations.

The distributions  $d\sigma/dE_T^{jet}$  and the number of jets versus the laboratory jet angle are shown in Fig. 4, separately for the current and target region, and

compared with CDM. Clearly more jets are produced in the target region compared to the current region. Generally the model describes the laboratory jet angle distribution for jets in the current region well. In the target region, particularly at small jet angles, the agreement is worse. The model clearly produces too few forward jets with a laboratory angle less than  $20^\circ$ .

Next, the  $ep$  jet cross sections are shown versus the target momentum fraction. The events are classified as 1+1 and 2+1 jet events (the +1 indicates the proton remnant which is generally not reconstructed). For the 1+1 jet events, i.e. the current jet + the proton remnant, the relevant target momentum fraction is the Bjorken- $x$ . The jets of these events are predominately found in the current region of the Breit frame. For 2+1 jet events the jets are found mostly in the target region. Here the relevant target momentum fraction is  $\xi$ , defined as  $\xi = x(Q^2 + M_{jj}^2)/Q^2 > x$ , where  $M_{jj}$  is the mass of the 2 jets. The data are shown in Fig.5 for the 1+1 and 2+1 jet sample, and compared with the CDM and MEPS predictions. Again a good description is found for the data in the current region, while an excess of data with respect to the Monte Carlo calculation is observed in the target region. This excess is found to result predominantly from  $\xi$  values in the region  $0.01 < \xi < 0.1$ , i.e. at relatively large target momentum fractions. The disagreement is larger for the MEPS model. BFKL dynamics would lead to produce more jets at relatively large  $\xi$  values, but other mechanisms to explain this excess cannot be excluded yet.

## 5. Conclusions

In order to shed light on the QCD mechanism responsible for parton evolution in the regime of small Bjorken- $x$ , the production of jets in the forward region has been measured at HERA.

A forward jet selection designed to enhance the yield in the case of BFKL evolution, and to suppress the yield for DGLAP evolution, results in a rate of observed forward jets compatible with the BFKL expectation. The H1 data show an excess of forward jet production compared to model calculations based on MEPS. The agreement with CDM in the selected kinematical range is good, but gets worse if the  $x_{jet}$  cut is increased. The ratio of the jet rate at small  $x$  to the one at large  $x$  is compatible with the expectations of BFKL dynamics. A firm conclusion on the growth with  $x$  however necessitates a larger data sample.

The inclusive jet cross section measurement from the ZEUS collaboration shows that there is a clear excess of forward jets compared to the model predictions. This excess is in the region of target momentum fraction where effects of the BFKL dynamics can be expected.

The results presented here are encouraging and

hint that BFKL dynamics may reveal itself in future measurements of this kind. To reach a firm conclusion, not only more data is needed, but also a (continuing) close collaboration between experiment and theory. The "shopping list" contains cross sections at the parton-jet level, higher order BFKL and DGLAP calculations for the phase space of these measurements, a BFKL based Monte Carlo program, more fundamental understanding of the remnant fragmentation...

## References

- [1] J. Bartels and J. Feltesse, Proc. of the Workshop on Physics at HERA, Hamburg 1991, eds. W. Buchmüller and G. Ingelman, vol. 1, p. 131;
- E.M. Levin, Proc. QCD - 20 Years Later, Aachen 1992, eds. P.M. Zerwas, H.A. Kastrup, vol. 1, p. 310.
- [2] ZEUS Collab., M. Derrick et al., Z. Phys. C65 (1995) 379.
- [3] H1 Collab.; T. Ahmed et al., Nucl. Phys. B439 (1995) 471.
- [4] Yu. L. Dokshitzer, Sov. Phys. JETP 46 (1977) 641;
- V.N. Gribov and L.N. Lipatov, Sov. J. Nucl. Phys. 15 (1972) 438 and 675;
- G. Altarelli and G. Parisi, Nucl. Phys. 126 (1977) 297.
- [5] E.A. Kuraev, L.N. Lipatov and V.S. Fadin, Sov. Phys. JETP 45 (1972) 199;
- Y.Y. Balitsky and L.N. Lipatov, Sov. J. Nucl. Phys. 28 (1978) 282.
- [6] A.J. Askew, J. Kwieciński, A.D. Martin, P.J. Sutton, Phys. Lett. B325 (1994) 212.
- [7] H1 Collab., S. Aid et al., DESY 95-081 (1995).
- [8] G. Marchesini, B.R. Webber, Nucl. Phys. B349 (1991) 617.
- [9] A.H. Mueller, Nucl. Phys. B (Proc. Suppl.) 18C (1990) 125;
- J. Phys. G17 (1991) 1443.
- [10] J. Kwieciński, A.D. Martin, P.J. Sutton, Phys. Rev. D46 (1992) 921.
- [11] A.H. Mueller, Columbia preprint CU-TP-658 (1994).
- [12] J. Bartels, H. Lotter, Phys. Lett. B309 (1993) 400.
- [13] J. Bartels, A. De Roeck, M. Loewe, Z. Phys. C54 (1992) 635;
- W.K. Tang, Phys. Lett. B278 (1992) 363.
- [14] L. Lönnblad, Computer Phys. Comm. 71 (1992) 15.
- [15] G. Gustafson, Ulf Petterson, Nucl. Phys. B306 (1988);
- G. Gustafson, Phys. Lett. B175 (1986) 453;
- B. Andersson, G. Gustafson, L. Lönnblad, Ulf Petterson, Z. Phys. C43 (1989) 625.
- [16] G. Ingelman, Proc. of the Workshop on Physics at HERA, Hamburg 1991, eds. W. Buchmüller and G. Ingelman, vol. 3, p. 1366.
- [17] L. Lönnblad, Z. Phys. C65 (1995) 285;
- A. H. Mueller, Nucl. Phys. B415 (1994) 373;
- L. Lönnblad, CERN-TH/95-95.
- [18] T. Sjöstrand, Comp. Phys. Comm. 39 (1986) 347;
- T. Sjöstrand and M. Bengtsson, Comp. Phys. Comm. 43 (1987) 367;
- T. Sjöstrand, CERN-TH-6488-92 (1992).
- [19] H1 Collab., I. Abt et al., "The H1 detector at HERA", DESY 93-103 (1993).
- [20] H1 Collaboration, S. Aid et al., DESY-95-108 (1995);
- J. Kurzhöfer, Ph.D. thesis, Universität Dortmund (1995).
- [21] V. Del Duca, talk at the Workshop on Deep Inelastic Scattering and QCD, Paris 1995 (to appear in the proceedings); M. Wüsthoff, private communication.
- [22] ZEUS Collaboration, The ZEUS Detector, Status Report 1993 DESY (1993).
- [23] S. Catani, Yu.L. Dokshitzer and B.R. Webber, Phys. Lett. B285 (1992) 291.

